Evaluation of OFDM-MIMO Systems Using Convolution with CPM

Guowei Lei, Sunqing Su*
School of Science, Jimei University, Xiamen 361021, P.R.China.

* Corresponding author. Tel. 13860141760; email: sunqingsu@126.com
Manuscript submitted September 10, 2019; accepted November 8, 2019.
doi: 10.17706/ijcce.2020.9.2.78-86

Abstract: Orthogonal frequency division multiplexing (OFDM) is regarded as a popular technique. Moreover, OFDM combined with multiple-input multiple-output systems (MIMO) has drawn many interests. However, OFDM-MIMO systems with continuous phase modulation have not been investigated extensively to date. In this paper, we propose an OFDM-MIMO system using convolution codes with continuous phase modulation (CPM). In the system, an interleaver is added between encoder and modulator. Moreover, iterative decoding and demodulation are combined together at receiver. To evaluate the performances, the comparisons between CPM and linear modulations in terms of bit error rate (BER), peak-to-average power ratio (PAPR) and power spectrum density (PSD) are given in the end.

Key words: OFDM, MIMO, continuous phase modulation, interleaver.

1. Introduction

Orthogonal frequency division multiplexing (OFDM) is a popular technique for transmission of signals over frequency-selective fading channel. In addition, OFDM offers good ability to combat multipath fading without complex equalization filters. In literatures, OFDM systems that employ linear and memory-less modulations such as PSK, QAM, etc, have been investigated extensively [1], [2]. On the other hand, continuous phase modulation (CPM) is a promising technology for its features such as constant envelope and phase continuity. Its constant envelope makes it more suitable for low cost non-linear power amplifier, its phase continuity makes it easily demodulated via phase trellis diagram. Moreover, the advantage that OFDM-CPM system brings to us is that adjacent OFDM symbols can be modulated by modulation index of CPM. Therefore, OFDM-CPM system has been proposed and studied owing to the above advantages [3]-[7]. The detection of OFDM-CPM signals is studied in [5], [6]. Peak-average power ratio (PAPR) is analyzed in OFDM-CPM systems [7].

Further, the performance of OFDM-CPM with multiple antennas is also studied [8]-[10]. The authors demonstrate that OFDM-MIMO with CPM offers considerable improvement relative to conventional OFDM-MIMO systems with linear modulations (PSK, QAM, etc.) [8]. To harness diversity gain, a kind of STBC scheme is introduced in OFDM-CPM systems [9]. To achieve low PAPR while maintaining robustness to frequency selective fading, the multiple modulation indices are introduced in OFDM-CPM system [10].

To date, many literatures have proposed the combination of channel codes with CPM due to the inner coding of continuous phase encoding (CPE). One of the most popular schemes is to employ convolution codes [11]. Under the same condition, encoding in OFDM-MIMO systems can improve the performance

without extra transmission power [12]. In this paper, we proposed a kind of OFDM-MIMO system using convolution codes with CPM. Meanwhile, the interleaver is added into the system to mitigate the chance of burst error caused by channel. Generally, iterative decoding is mostly used in Turbo-CPM systems [13], [14]. To simplify the decoding algorithm without sacrificing the performance, iterative decoder and demodulator are combined together for convolution and CPM. In addition, multiple modulation indices are considered in CPM scheme to improve peak-to-average power ratio (PAPR). In the end, simulated results are given to validate our proposed system.

The rest of this article is organized as follows. The proposed system is briefly described in Section II. The transmit model and receive model are introduced respectively. In Section III, simulated results are presented and discussed. Finally, the work is concluded in Section IV.

2. System Model

The system is described in Fig. 1. At the transmit side, serial input symbols are de-multiplexed into several parallel branches. Each branch is encoded with convolution. After convolution, these branches are multiplexed and interleaved. And then they are de-multiplexed again into several parallel branches. Finally, each branch is modulated as CPM signal, and further modulated as OFDM signal. The parallel signals are transmitted simultaneously from several antennas. At the receive side, the OFDM signals are de-multiplexed again into parallel branches. Then, each branch is demodulated into symbols. Finally, the symbols are de-interleaved and decoded into information stream.

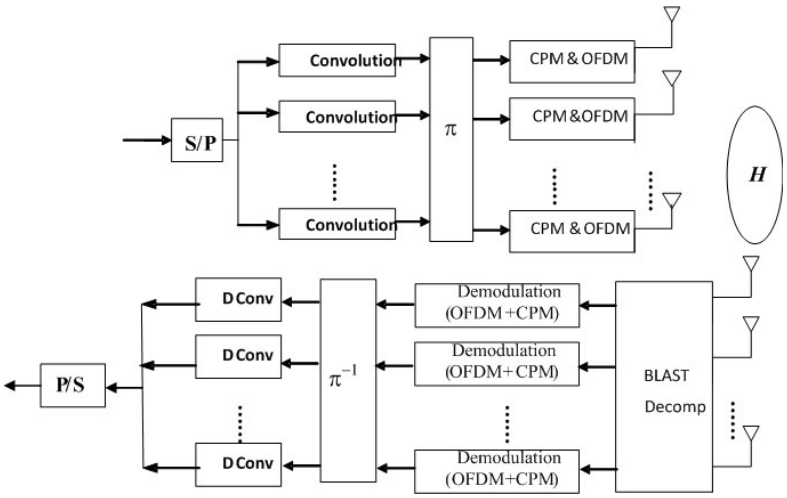

Fig. 1. System model of OFDM-MIMO with CPM.

2.1. Transmitter Model

We denote channel coefficients as $\boldsymbol{H}_{Nr\times Nt}$. And h_{nrnt} denotes each entry of channel matrix $\boldsymbol{H}_{Nr\times Nt}$, where N_r is the number of receive antennas, N_t is the number of transmit antennas, $w(t)$ denotes added white Gaussian noise (AWGN) with variance $2N_0$. With these assumptions, the received signals can be represented as

$$r_{n_r}(t;D_{\mathrm{p,k}}) = \sum_{n_t=1}^{N_t} h_{n_r n_t} \mathrm{s}(t;D_{\mathrm{p,k}}) + w_{n_r}(t) \qquad n_r=1,\ldots,N_r \tag{1}$$

As is well known, OFDM with linear modulations has been investigated extensively. In this paper, more attention is paid to CPM-OFDM modulated signals. Without loss of generality, the CPM mapper/modulator is hereby defined as [3]

$$C_{\mathrm{p,k}} = cos(\theta_{\mathrm{p,k}}) + \mathrm{j}\, sin(\theta_{\mathrm{p,k}}) \tag{2}$$

and

$$\theta_{\mathrm{p,k}} = D_{\mathrm{p,k}} \pi h_{\mathrm{p}} + \pi h_{\mathrm{p}} \sum_{\mathrm{q}=0}^{\mathrm{p}-1} D_{\mathrm{q,k}} + \varphi \tag{3}$$

where h_{p} is modulation index, $D_{p,k}$ is M-ary CPM symbol drawn from {±1,±3,...,±(M-1)}, p=1,2,..., and k=0,...,N-1. It is noted that p denotes the OFDM block number and k denotes the subcarrier number. φ is the initial phase.

Further, the OFDM signals are given by

$$s(t; D_{\mathrm{p,k}}) = \sum_{k} \sum_{p} \mathrm{C}_{\mathrm{p,k}} g(t - kT) \mathrm{e}^{j(2\pi/T)pt}, \quad 0 \le t < \infty \tag{4}$$

where

$$\mathrm{g}(t) = \begin{cases} \dfrac{1}{\sqrt{T}} & 0 \le t \le LT \\ 0 & \text{elsewhere} \end{cases} \tag{5}$$

In (4) and (5), T is symbol duration of CPM, L=1 is for full response signaling. More specifically, h_p=h/p where h and p are positive integer numbers and integer values for h_p are forbidden [15]. Meanwhile, a correct definition of the modulation index requires that h and p are relative prime to have a minimal trellis representation. In multiple h_p CPM, the value of h_p is selected from [1/8, 7/8], depending on whether data bit is changed or not. For example, if data bit is not changed, *e.g.* from '0' to '0', or from '1' to '1', then h_p=1/8, if data bit is changed from '0' to '1', or from '1' to '0, then h_p=7/8. Since m is odd, we know that the constellation distribution for h_p=1/8 and h_p=7/8 should be same [16], including the total number of constellation. In Fig. 2, we can see the number of constellation for h_p=1/8 and h_p=7/8 is 16.

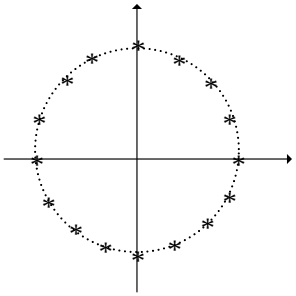

Fig. 2. The constellation diagram of CPM symbols for h_p=1/8 and h_p=7/8.

The PAPR of the transmitted signal in (4) can be defined as

$$\mathrm{PAPR} = \frac{max\left|s(t)\right|^2}{E\left[\left|s(t)\right|^2\right]} \tag{6}$$

The theorem of convolution codes is to encode one or k bits and output n bits. Generally, it can be expressed as (n, l, m), where n denotes the number of encoder flag, l denotes the length of input symbols, m denotes the number of sequential registers. The coding rate R is hereby l/n. In Fig. 3, M=2 and M=4 are respectively denoted as binary and quaternary encoders. In (a), the encoder is comprised of one input port,

three shift registers, two modulo by 2 adders and two output ports, which can be expressed with generator matrix $G(D)$=[1+D+D^2, 1+ D^2]. In (b), the encoder is comprised of one input port, three shift registers, three modulo by 4 adders and three output ports, which can be expressed with generator matrix $G(D)$=[1+D+D^2, 1+D^2, D+D^2]. Hence, binary and quaternary encoders are compatible and linked with CPM with M=2 and M=4 respectively.

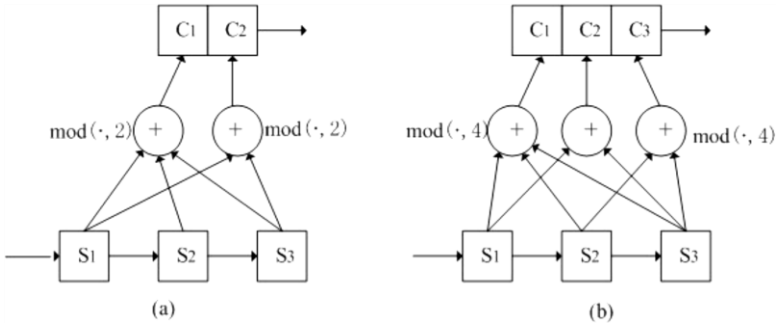

Fig. 3. The structures of convolution coder for M=2 and M=4.

The role of interleaver in communication systems is to solve the burst errors of sequences in the transmission process. The first function of interleaver is to scramble the data sequences, and then correct these errors by convolution codes. The second function of interleaver is to be put in the inner coder and the external coder. There will be potential errors in the output of the external decoder. The errors are randomly distributed by the interleaver, such that the errors of the inner decoder are random, hereby ensuring the effect of the inner coder. The performance of random interleaver is excellent, especially when the length of interleaver is longer.

2.2. Receiver Model

It is assumed that the channel state information (CSI) can be obtained via channel estimation. At the receiver, several detection algorithms, *e.g.* Zero-Forcing (ZF) or Minimum Mean Square Error (MMSE) can be employed. Hereby we choose MMSE and obtain the decoupled signals as follows

$$\hat{\boldsymbol{s}}(t) = \left(\boldsymbol{H}^{\mathrm{H}}\boldsymbol{H} + N_0\boldsymbol{I}\right)^{-1}\boldsymbol{H}^{\mathrm{H}}\boldsymbol{r}(t) + \boldsymbol{H}^{\mathrm{H}}\boldsymbol{w}(t) \tag{7}$$

Then, we employ maximum likelihood (ML) detection to get $C_{p,k}$ as follows

$$\hat{\boldsymbol{C}}_{p,k} = \underset{\hat{C}_{p,k}}{argmin}\left|\hat{\boldsymbol{s}}(t; D_{\mathrm{p,k}}) - \sum_{k}\sum_{p}\boldsymbol{C}_{p,k}\,g(t-kT)\boldsymbol{e}^{j(2\pi/T)pt}\right|^2 \tag{8}$$

The pair wise probability (PEP) conditioned onto fading channel statistics can be written as follows [17]

$$p(\boldsymbol{S} \to \hat{\boldsymbol{S}} \mid \boldsymbol{H}) = \boldsymbol{Q}\left(\sqrt{\frac{\boldsymbol{E}_s}{2\boldsymbol{N}_0}\left\|\boldsymbol{H}(\boldsymbol{S}-\hat{\boldsymbol{S}})\right\|^2}\right) \tag{9}$$

Plugging the right terms of (8) into (9), we can obtain as follows

$$p(\boldsymbol{S} \to \hat{\boldsymbol{S}} \mid \boldsymbol{H}) = \boldsymbol{Q}\left(\sqrt{\gamma\left\|\boldsymbol{H}\left(\hat{s}(t; D_{\mathrm{p,k}}) - \sum_{k}\sum_{p}\boldsymbol{C}_{p,k}\,g(t-kT)\boldsymbol{e}^{j(2\pi/T)pt}\right)\right\|^2}\right) \tag{10}$$

where E_s is the power of OFDM signals, γ=E_s/2N_0 is the signal to noise ratio. $Q(\cdot)$ is the Q-function. In (9), the

PEP is determined by the *Euclidean* norm of OFDM signals.

Generally, the de-convolution (DConv) or the de-modulation (DCPM) can be performed via Viterbi algorithm or BCJR algorithm [18]. In this paper, we mainly consider the later, and try to combine the DConv and the DCPM and perform iterative decoding and demodulation. In Fig. 4, the iterative decoder consists of one a posteriori probability (APP) algorithm for CPM and the convolution encoder. The iterative decoding and demodulation utilize a priori probabilities of both information symbols and code symbols, and calculates extrinsic APP of both information symbols and code symbols. It is worth noting that, $C_{p,k}$ denotes the input of de-modulation, $I_{p,k}$ denotes the output stream of de-convolution. $\lambda_{p,k}$ denotes the soft information for the output of de-convolution, $\pi(\lambda_{p,k})$ denotes its interleaving. $\eta_{p,k}$ denotes the soft information for the input of de-convolution, $\pi(\eta_{p,k})$ denotes its interleaving. For M=2, the soft information such as $\lambda_{p,k}$, $\eta_{p,k}$ should fulfill as follows

$$\begin{aligned}\lambda_{p,k}\left(D_{p,k}=+1\right)+\lambda_{p,k}\left(D_{p,k}=-1\right)=1\\ \eta_{p,k}\left(D_{p,k}=+1\right)+\eta_{p,k}\left(D_{p,k}=-1\right)=1\end{aligned} \tag{11}$$

For M=4, the soft information such as $\lambda_{p,k}$, $\eta_{p,k}$ should fulfill as follows

$$\begin{aligned}\lambda_{p,k}\left(D_{p,k}=+3\right)+\lambda_{p,k}\left(D_{p,k}=+1\right)+\lambda_{p,k}\left(D_{p,k}=-1\right)+\lambda_{p,k}\left(D_{p,k}=-3\right)=1\\ \eta_{p,k}\left(D_{p,k}=+3\right)+\eta_{p,k}\left(D_{p,k}=+1\right)+\eta_{p,k}\left(D_{p,k}=-1\right)+\eta_{p,k}\left(D_{p,k}=-3\right)=1\end{aligned} \tag{12}$$

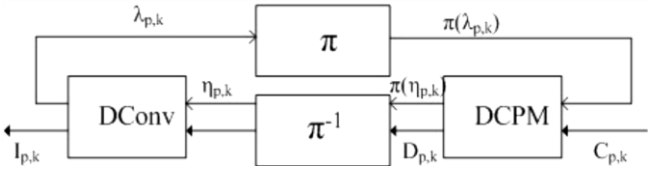

Fig. 4. Iterative decoder and demodulator for convolution and CPM.

3. Simulation and Analysis

In this section, we give Monte-Carlo simulations for the OFDM-MIMO system using convolution with CPM. For convenience, the proposed system with N_t=4, N_r=4 is evaluated as an instance. Each spatial channel is modeled to be independent and *Rayleigh* fading. First, we assume that the channel is polluted by the noise w with zero-mean and variance $2N_0$.

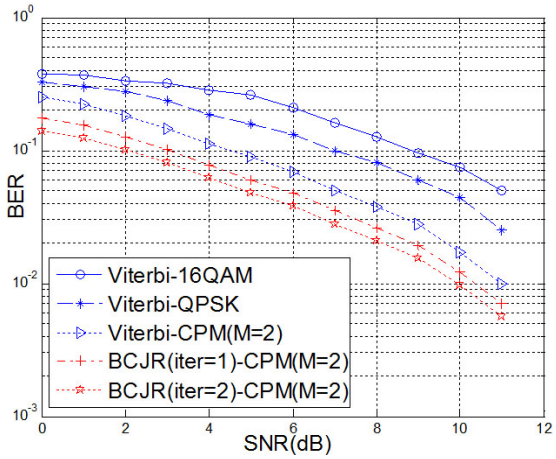

Fig. 5. Comparison among various modulations and detections in OFDM-MIMO systems.

We provide the comparison among various modulations and detections in OFDM-MIMO systems. The phase smoothing function of CPM signal takes the form of LRET full response (L=1) with h_p=1/4 and M=2. In Fig. 5, it is shown that, CPM has the best bit error ratio (BER) performances among these modulations, and QPSK has 2dB performance over 16QAM via Viterbi algorithm. In addition, BCJR algorithm performs better than Viterbi algorithm. As the number of iteration increases, the BER performance improves a litter.

We provide the comparison between interleaving and non-interleaving with modulations in OFDM-MIMO systems. The phase smoothing function of CPM signal takes the form of LRET full response (L=1) with h_p=1/4 and M=2. In Fig. 6, it is shown that, CPM has the better BER performances than QPSK. The interleaver can bring the improvement of 1dB performance for both CPM and QPSK. In addition, BCJR algorithm performs better than Viterbi algorithm.

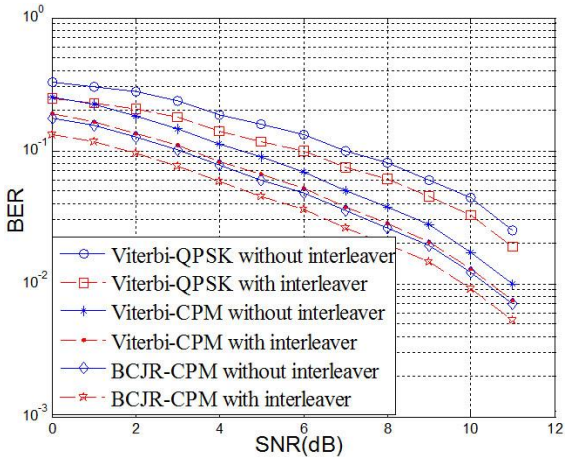

Fig. 6. Comparison between interleaving and non-interleaving in OFDM-MIMO systems.

We provide the comparison for CPM with various modulation formats in OFDM-MIMO systems. In Fig. 7, it is shown that CPM with h_p=1/2 performs better than CPM with h_p=1/4, which is attributed to the constellation of CPM symbols, since the *Euclidean* distance of CPM with h_p=1/2 is bigger than its counterpart with h_p=1/4. Likewise, it is shown that CPM with M=2 performs better than CPM with M=4, which can be inferred from (10) and (11).

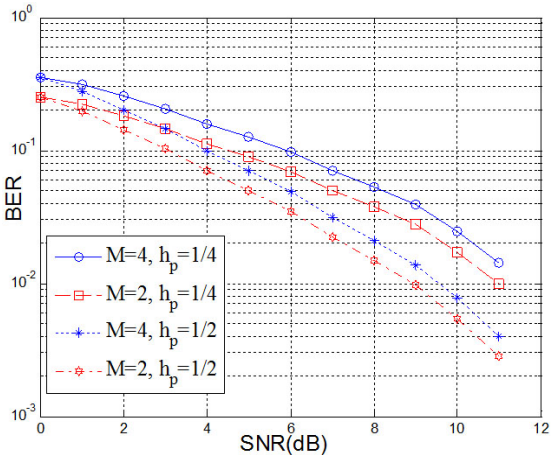

Fig. 7. Comparison for CPM with various modulation formats in OFDM-MIMO systems.

We provide the comparison of complementary cumulative distribution (CCD) function of 256-subcarrier OFDM-MIMO system for various modulations. The simulation is run 1000 OFDM blocks and the transmitted

signal is oversampled by the factor of four, which is sufficient to capture the peaks. In Fig. 8, it can be seen that the PAPR for OFDM-MIMO with multi-h_p CPM is better than that for OFDM-MIMO with BPSK. Meanwhile, the PAPR for OFDM-MIMO with h_p=1/4 CPM is close to the OFDM-MIMO with QPSK. On the other hand, the PAPR for OFDM-MIMO with 16QAM is the worst among these modulations.

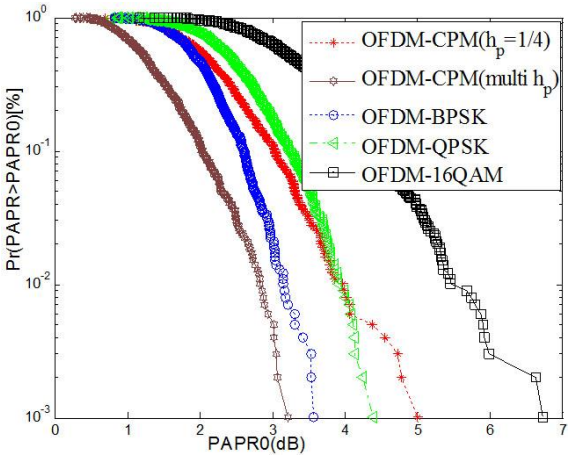

Fig. 8. Complementary cumulative distribution function of 256-subcarrier OFDM-MIMO system for various modulations.

We provide the comparison of the power spectrum density (PSD) of 256-subcarrier OFDM-MIMO system for various modulations. In Fig.9, it is shown that the main lobe of OFDM-MIMO with multi-h_p CPM is flat than that of OFDM-MIMO with BPSK and 16QAM, while the side lobe of OFDM-MIMO with multi-h_p CPM is lower than for OFDM-MIMO with h_p=1/4 CPM. It is demonstrated that OFDM-MIMO with multi-h_p CPM gives excellent bandwidth efficiency.

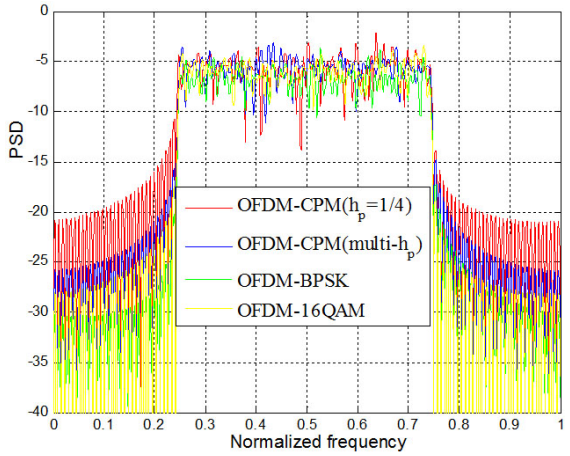

Fig. 9. PSD of 256-subcarrier OFDM-MIMO system for various modulations.

4. Conclusions

In this paper, we propose the OFDM-MIMO system using convolution codes with continuous phase modulation. In the system, the interleaver is added between encoder and modulator. Moreover, iterative decoding and demodulation are combined together at receiver, where multiple format modulated signals are suitable for transmission without any complexity of hardware or computation. To evaluate the performances, we have provided the comparison between CPM and other linear modulations. It can further

be declared that, multiple modulation indices can improved the performances such as PAPR and PSD. In future, we would like to investigate the OFDM-MIMO systems using polar codes with CPM. As is well known, polar codes have been considered a good standard of channel coding for next generation of wireless communications [19].

Conflict of Interest

The authors declare that there is no conflict of interest for writing and publication of the paper.

Author Contributions

Lei Guowei is responsible for the design of the proposed system, some derivations and simulations; Su Sunqing is responsible for the writing and check of the paper; all authors have approved the final version.

Acknowledgment

This work was supported in part by Foundation project of department of education of Fujian Province (JAT160260), Li Shangda Discipline Construction Fund (ZC2016008), and Research Start-up Fund of Jimei University (ZQ2019021).

References

[1] Cai, X. D., & Giannakis, G. B. (2004). Error probability minimizing pilots for OFDM with M-PSK modulation over Rayleigh-fading channels. *IEEE Transactions on Vehicular Technology*, *53(1)*, 146-155.

[2] Montojo, J. I., & Milstein, L. B. (2011). Error rate for PSK and QAM modulations for non-ideal OFDM Systems with noisy channel estimates and receive diversity. *IEEE Transactions on Communications*, *59(10)*, 2703-2715.

[3] Tasadduq, I. A., & Rao, R. K. (2002). OFDM-CPM signals. *Electronics Letters*, *38(2)*, 80-81.

[4] Tasadduq, I. A., & Rao, R. K. (2003). OFDM-CPM signals for wireless communications. *Canadian Journal of Electrical and Computer Engineering*, *28(1)*, 19-25.

[5] Shafter, E., Alsharef, M., & Rao, R. K. (2016). Detection of M-ary OFDM systems with CPM mapper over multipath Channels. *Proceedings of the IEEE 21st International Workshop on Computer Aided Modeling and Design of Communication Links and Networks (CAMAD)* (pp. 107-111). Toronto, CA.

[6] Tasadduq, I. A., & Rao, R. K. (2003). Viterbi decoding of OFDM-CPM signals. *The Arabian Journal for Science and Engineering*, *28(2)*, 71-80.

[7] Tasadduq, I. A., & Rao, R. K. (2002). PAPR reduction of OFDM signals using multiamplitude CPM. *Electronics Letters*, *38(16)*, 915-917.

[8] Clara, R. I., & Rao, R. K. (2005). OFDM-CPM for MIMO wireless communication: Signal detection and performance. *Proceedings of the Canadian Conference on Electrical and Computer Engineering* (pp. 1388-1391). Saskatoon, CA.

[9] Mohamed, E. K., Mohamed, H. G., & Badawy, E.-S. A. (2012). Achieving higher throughput in STBC-OFDM systems using non-linear modulation techniques. *Proceedings of the IEEE Symposium on Wireless Technology and Applications* (pp. 38-42). Bandung, Indonesia.

[10] Hisojo, M. A., Lebrun, J., & Deneire, L. (2014). Zero-forcing approach for L2-orthogonal ST-codes with CPM-OFDM schemes and frequency selective Rayleigh fading channels. *IEEE Military Communications Conference*, 563-568.

[11] Zhang, L., Chen, T., & Wang, H. B. (2010). Trellis analysis for convolutional coded continuous phase modulation over rings. *Proceedings of the 2010 2nd International Conference on Computer Engineering and Technology* (pp. 393-396). Chengdu, China.

[12] Astawa, I. G. P., Moegiharto, Y., Zainudin, A., *et al*. (2014). Performance of MIMO-OFDM using convolution codes with QAM modulation. *Proceedings of the 6th International Conference on Digital Image Processing (ICDIP 2014)* (pp. 915-90F). Athens, Greece.

[13] Majoobi, L., & Mohammadi, A. (2009). Continuous phase modulation detection using TURBO-BLAST. *Proceedings of the Wireless VITAE'2009* (pp. 212-216). Denmark.

[14] Xue, R., Zhao, D. F., & Zhu, T. L. (2008). An improved method for the convergence of iterative detection in turbo-CPM system. *Computer Simulation*, *26(6)*, 141-145.

[15] Mazzali, N., Colavolpe, G., & Buzzi, S. (2013). CPM-based spread spectrum systems for multi-user communications. *IEEE Transactions on Wireless Communications, 12(1)*, 358-367.

[16] Anderson, J. B., Aulin, T., & Sundberg, C.-E. W. (1986). *Digital Phase Modulation*. NY, US: Springer.

[17] Lei, G. W., Liu, Y. A., & Xiao, X. F. (2003). Performance analysis of adaptive space-time coded systems with continuous phase modulation. *AEU-International Journal of Electronics and Communications*, *80(2017)*, 80-85.

[18] Bahl, L., Cocke, J., Jelinek, F., & Raviv, J. (1974). Optimal decoding of linear codes for minimizing symbol error rate. *IEEE Transactions on Information Theory*, *20(2)*, 284-287.

[19] Cyriac, A., & Narayanan, G. (2018). Polar code encoder and decoder implementation. *Proceedings of the 3rd International Conference on Communication and Electronics Systems (ICCES)*.

Guowei Lei received the B.S. degree in physics from Gannan Normal University in 1999, the M.S. degree in electronics from Xiamen University in 2004, the Ph.D degree in electronics from Beijing University of Posts and Telecommunications in 2019, respectively. Since 2004, he is with School of Science, Jimei University, Xiamen, China. His interests include the signal processing in wireless communications.

Sunqing Su received the B.S. degree in physics from Fujian Normal University in 1985. Since 2006, he is with School of Science, Jimei University, Xiamen, China. His interests include the quantum communications.